

# Oscillating solutions of the Vlasov-Poisson system—A numerical investigation

Tobias Ramming, Gerhard Rein  
 Fakultät für Mathematik, Physik und Informatik  
 Universität Bayreuth  
 D-95440 Bayreuth, Germany  
 email: tobias.ramming@uni-bayreuth.de  
 gerhard.rein@uni-bayreuth.de

April 14, 2016

## Abstract

Numerical evidence is given that spherically symmetric perturbations of stable spherically symmetric steady states of the gravitational Vlasov-Poisson system lead to solutions which oscillate in time. The oscillations can be periodic in time or damped. Along one-parameter families of polytropic steady states we establish an Eddington-Ritter type relation which relates the period of the oscillation to the central density of the steady state. The numerically obtained periods are used to estimate possible periods for typical elliptical galaxies.

## 1 Introduction

In astrophysics, a large ensemble of stars such as a galaxy or a globular cluster is often modelled as a self-gravitating collisionless gas which obeys the Vlasov-Poisson system

$$\partial_t f + v \cdot \nabla_x f - \nabla U \cdot \nabla_v f = 0, \quad (1.1)$$

$$\Delta U = 4\pi\rho, \quad \lim_{|x| \rightarrow \infty} U(t, x) = 0, \quad (1.2)$$

$$\rho(t, x) = \int f(t, x, v) dv. \quad (1.3)$$

Here  $f = f(t, x, v) \geq 0$  is the number density of the ensemble in phase space and depends on time  $t \in \mathbb{R}$ , position  $x \in \mathbb{R}^3$ , and velocity  $v \in \mathbb{R}^3$ ,  $\rho$  is

the spatial mass density induced by  $f$ —unless explicitly stated otherwise integrals always extend over  $\mathbb{R}^3$ —, and  $U$  is the gravitational potential generated by the ensemble. We assume that all the particles, i.e., stars, in the ensemble have the same mass which we normalize to unity. We refer to [2] for the astrophysics background of this system.

The initial value problem for the Vlasov-Poisson system is well understood, and smooth initial data launch global smooth solutions, cf. [13, 17, 21] or the review article [19]. The system is known to have a plethora of steady states. The spherically symmetric ones can be obtained by the following approach. If the potential  $U$  is time-independent and spherically symmetric, then the particle energy and the angular momentum squared,

$$E = E(x, v) := \frac{1}{2}|v|^2 + U(x), \quad L := |x \times v|^2, \quad (1.4)$$

are constant along particle orbits, i.e., along solutions of the characteristic system

$$\dot{x} = v, \quad \dot{v} = -\nabla U(x)$$

of the Vlasov equation (1.1). Hence an ansatz of the form

$$f = \phi(E, L) \quad (1.5)$$

satisfies the Vlasov equation and reduces the system to a semilinear Poisson equation for  $U$ , which is obtained from (1.2) by substituting the ansatz into the definition (1.3) of the spatial density. The question which ansatz functions  $\phi$  lead to steady states which have finite total mass and extension has been investigated by several authors, and we refer to [18] and the references there. We will denote steady state quantities by  $f_0$ ,  $U_0$ , etc. Of obvious interest from the mathematics as well as applications point of view is the nature of the dynamics in a neighborhood of such a steady state. What is by now well understood is that these steady states are stable provided  $\phi$  is a strictly decreasing function of the energy  $E$  on the support of the steady state; for precise formulations of such stability results we refer to [4, 5, 6, 12, 19] and the references there.

However, the fact that a particular steady state is stable does not tell us the dynamical behavior of solutions which are launched by small perturbations of it. This is the issue we study in the present paper by numerical means. The somewhat surprising observation is that all spherically symmetric and not too large perturbations of a given stable steady state seem to launch solutions which oscillate in time in the sense that their kinetic and potential energies oscillate and their spatial support continues to expand and

contract. These oscillations can be time-periodic or damped, depending on the steady state which is perturbed. Such a behavior was already noticed in [1] for the Einstein-Vlasov system. We have for the Vlasov-Poisson system investigated these oscillations with much higher numerical precision, for much longer time spans and in a more systematic way. We believe that they constitute an interesting new building block for the picture of the overall dynamical possibilities of the Vlasov-Poisson system, and to understand these time-periodic oscillations in a mathematically rigorous way is a challenging and worthwhile problem in mathematical physics, cf. [7].

Our numerical results should be compared with the one-parameter family of semi-explicit solutions constructed by KURTH [10]. Here the spatial density is at each time constant on a ball of radius  $R(t)$  and zero elsewhere, and the free parameter of the family is  $\dot{R}(0)$ . If  $\dot{R}(0) = 0$ , the solution is a steady state, and if  $0 < |\dot{R}(0)| < 1$ , then the function  $R$  and hence the whole solution is time periodic with the amplitude of the oscillations going to zero as  $\dot{R}(0)$  goes to zero. One can sum up the findings of our investigation by saying that up to possible damping the Kurth family captures the generic picture of the dynamics in a neighborhood of any stable steady state, provided we restrict ourselves to spherical symmetry.

The paper proceeds as follows. In the next section we reformulate the system in coordinates adapted to spherical symmetry, and we discuss the type of steady states which we perturb and the numerical approach used in our investigation. In Section 3 we present our numerical observations of oscillating solutions. We explain the various diagnostics which were employed to numerically test the time-periodicity, present some typical results which exhibit this property, and we investigate the relation between the amplitude and frequency of the oscillations. We find that in the limit of small perturbations the frequency of the oscillations does not depend on the type of perturbation but only on the perturbed steady state. In Section 4 we consider one-parameter families of steady states given by a fixed polytropic ansatz function and study the dependence of the period of oscillation on the parameter which can be chosen as the central density of the steady state. Such a relation is known for polytropic fluid models of stars. In the present context it generalizes also to the unisotropic states. In Section 5 we briefly consider the question for which steady states the oscillations seem to be damped and for which they seem to be undamped and truly time periodic. We conclude with some final discussion of our observations in the last section.

## 2 The spherically symmetric system and the numerical algorithm

By definition a distribution function  $f$  is *spherically symmetric* iff  $f(t, x, v) = f(t, Ax, Av)$  for all rotations  $A \in \text{SO}(3)$ . By uniqueness, spherically symmetric initial data launch spherically symmetric solutions. A spherically symmetric distribution function can be written in the form  $f = f(t, r, w, L)$  where

$$r := |x|, \quad w := \frac{x \cdot v}{r}, \quad L := |x \times v|^2;$$

$w$  is the radial velocity, and  $L$ , the modulus of angular momentum squared, is conserved along particle trajectories due to spherical symmetry. In these variables the Vlasov-Poisson system takes the form

$$\partial_t f + w \partial_r f + \left( \frac{L}{r^3} - \partial_r U(t, r) \right) \partial_w f = 0, \quad (2.1)$$

$$\partial_r U(t, r) = \frac{m(t, r)}{r^2}, \quad (2.2)$$

$$m(t, r) = 4\pi \int_0^r \rho(t, s) s^2 ds, \quad (2.3)$$

$$\rho(t, r) = \frac{\pi}{r^2} \int_{-\infty}^{\infty} \int_0^{\infty} f(t, r, w, L) dL dw. \quad (2.4)$$

Here we have integrated the spherically symmetric Poisson equation once and have put it into a form which is numerically easy to deal with.

As pointed out in the introduction there is a plethora of steady states of the Vlasov-Poisson system. We restrict the general ansatz to the technically convenient, more specific form

$$f = \phi(E_0 - E) (L - L_0)_+^l. \quad (2.5)$$

Here  $l > -1/2$ ,  $L_0 \geq 0$  is a cut-off angular momentum,  $E_0 < 0$  is a cut-off energy,  $\phi : \mathbb{R} \rightarrow [0, \infty[$  is measurable,  $\phi(\eta) = 0$  for  $\eta < 0$ , and  $\phi > 0$  a. e. on  $[0, \infty[$ , and  $(\cdot)_+$  denotes the positive part. If  $U_0 = U_0(r)$  denotes the potential of the spherically symmetric steady state to be constructed then  $y = E_0 - U_0$  satisfies an equation of the form

$$y' = -\frac{4\pi}{r^2} \int_0^r s^{2l+2} g(y(s)) ds \quad (2.6)$$

where  $g \in C(\mathbb{R}) \cap C^1(]0, \infty[)$  is determined by  $\phi$ , vanishes on  $] - \infty, 0]$ , and is strictly positive on  $]0, \infty[$ . For every prescribed value for  $y(0) > 0$  one

obtains a unique solution of (2.6) on  $[0, \infty[$ , and the corresponding steady state is compactly supported iff  $y$  has a zero, i.e.,  $y(R) = 0$  for some radius  $R > 0$ . In [18] and the references there one finds sufficient conditions on the ansatz function  $\phi$  for this to happen. The cut-off energy is then defined by  $E_0 = \lim_{r \rightarrow \infty} y(r)$ . In this way a fixed ansatz of the form (2.5) leads to a one-parameter family of steady states which is parameterized by  $y(0) = E_0 - U(0)$ , the potential energy difference between the center and the spatial boundary of the state.

We mention examples of steady state ansatz functions which play a role in our investigation:

**Polytropic balls.** Here

$$f_0 = (E_0 - E)_+^k L^l, \quad -1 < k < 3l + 7/2. \quad (2.7)$$

In this case the steady state is supported on a ball of radius  $R$ , and the steady state is isotropic or unisotropic depending on whether  $l = 0$  or  $l \neq 0$ .

**Polytropic shells.** Here

$$f_0 = (E_0 - E)_+^k (L - L_0)^l, \quad -1 < k < 3l + 7/2, \quad L_0 > 0. \quad (2.8)$$

In this case the steady state is supported on a shell with inner radius  $R_i = \sqrt{L_0/(2y(0))}$  and outer radius  $R > R_i$ , and the steady state is unisotropic.

**King's model.** Here

$$f_0 = (e^{E_0 - E} - 1)_+. \quad (2.9)$$

In this case the steady state is supported on a ball of radius  $R$  and isotropic. All these steady states have finite mass and compact support, and they are known to be stable.

**Kurth's model.** Here

$$f_0(x, v) = \frac{3}{4\pi^3} \begin{cases} (1 - |x|^2 - |v|^2 + L)^{-1/2}, & \text{where } (\dots) > 0 \text{ and } L < 1, \\ 0, & \text{else} \end{cases} \quad (2.10)$$

defines a steady state with spatial density and potential

$$\rho_0(x) = \frac{3}{4\pi} \mathbf{1}_{B_1}(x), \quad U_0(x) = \begin{cases} |x|^2/2 - 3/2, & |x| \leq 1, \\ -1/|x|, & |x| > 1; \end{cases}$$

notice that  $f_0$  is again a function of  $E$  and  $L$ . The importance of this model for the present investigation lies in the fact that the transformation

$$f(t, x, v) = f_0(x/R(t), R(t)v - \dot{R}(t)x)$$

turns this steady state into a time dependent solution with spatial mass density

$$\rho(t) = \frac{3}{4\pi} \frac{1}{R^3(t)} \mathbf{1}_{B_{R(t)}},$$

provided the function  $R = R(t)$  solves the differential equation

$$\ddot{R} - R^{-3} + R^{-2} = 0,$$

and  $R(0) = 1$ . The only free parameter in this family is  $\epsilon = \dot{R}(0)$ . For  $\epsilon = 0$  one recovers the steady state  $f_0$ , and for  $0 < |\epsilon| < 1$  the function  $R$  and hence the solution  $f$ , which for  $|\epsilon|$  small is a small perturbation of  $f_0$ , is time periodic with period  $2\pi(1 - \epsilon^2)^{-3/2}$ .

In our numerical simulations we used the following types of perturbations of such steady states:

- (P1) Perturbations by amplitude:  $\mathring{f} = (1 + \epsilon)f_0$  with  $\epsilon \in \mathbb{R}$  small.
- (P2) Perturbations by shift:  $\mathring{f} = f_0(\cdot + (r, w, L)_\epsilon)$  where the displacement vanishes as  $\epsilon \rightarrow 0$ .
- (P3) Kurth-type perturbations:  $\mathring{f}(x, v) = f_0(x, v - \epsilon x)$ .
- (P4) Dynamically accessible perturbations: During an initial time interval  $[0, t_{\text{pert}}]$  the initial data  $f_0$  is evolved under the influence of an external field  $\epsilon F$  or under the modified self-consistent field  $-(1 + \epsilon)\nabla U_0$ , and the perturbation  $\mathring{f}$  is defined as this evolved state evaluated at  $t = t_{\text{pert}}$ .

Perturbations of the latter type preserve all the Casimir invariants  $\int C(f) dv dx$  of the Vlasov-Poisson system.

For the numerical simulations we used a particle-in-cell scheme which we briefly review in the spherically symmetric set-up. Given spherically symmetric and compactly supported initial data  $\mathring{f}$  we initialize the scheme by splitting the support into a finite number of disjoint cells. Into each cell we place a numerical particle with a weight given by the volume of that cell times the value of  $\mathring{f}$  at the position of the particle. In the time step we take such a collection of particle positions and corresponding weights and compute from this an approximation of  $\rho$  and hence of  $m$  and  $\partial_r U$  on a grid in the radial direction. This grid is chosen such that it covers the  $r$ -interval in which the numerical particles are currently found. Using the approximation of  $\partial_r U$  the particle positions can now be updated by moving them according to the characteristic system of the Vlasov equation (2.1):

$$\dot{r} = w, \quad \dot{w} = \frac{L}{r^3} - \partial_r U(t, r), \quad \dot{L} = 0; \quad (2.11)$$

close to the origin it is advantageous to use Cartesian coordinates for propagating the particles. We found that a simple Euler scheme is sufficient for propagating the particles. The weights of the particles are not changed in the time step, which reflects the fact that the characteristic flow conserves phase space volume.

The conservation of the total mass  $\iint f(t, x, v) dv dx$  is a generic feature of this scheme. On the other hand, solutions of the Vlasov-Poisson system also conserve energy  $\mathcal{H} = E_{\text{kin}} + E_{\text{pot}}$ , the kinetic and potential parts of which are defined by

$$E_{\text{kin}}(t) = \frac{1}{2} \iint |v|^2 f(t, x, v) dv dx, \quad E_{\text{pot}}(t) = -\frac{1}{8\pi} \int |\nabla U(t, x)|^2 dx.$$

Conservation of energy is not built into the scheme and can hence be used to monitor its accuracy.

The above scheme is easy to parallelize. Each processor is responsible for a fixed batch of the numerical particles, i.e., for propagating them according to (2.11) and for computing their contribution to  $\rho$ . Of course at each time step these contributions have to be added up to obtain the total spatial density  $\rho$  and the induced field according to (2.2), but since the number of grid points of the spatial grid in the radial direction is very much smaller than the number of numerical particles, the scheme scales very well when the number of processors is increased, cf. [9].

### 3 Oscillating solutions

Since we want to numerically investigate the question whether or not small perturbations of steady states lead to oscillating behavior, it seems worthwhile to first test the employed particle-in-cell code on the family of Kurth solutions (2.10). As mentioned before, for  $0 < \epsilon < 1$  these solutions are time-periodic with period  $2\pi(1 - \epsilon^2)^{-3/2}$ . The numerically computed density profile of the solution for  $\epsilon = 0.2$  is presented in Figure 1(a); its potential energy as a function of time is shown in Figure 1(b). Table 1 shows the dependence of the period on the parameter  $\epsilon$  together with some corresponding numerical results. These match the theoretical predictions quite well. Also the discontinuity of the spatial density  $\rho$  at  $|x| = R(t)$  is recovered nicely. Given the fact that Lagrangian methods based on the strong formulation of the problem suffer seriously from low regularity and that for the Kurth solutions  $\rho$  is discontinuous and  $f$  singular at the boundaries of their respective supports, the code passes this test quite well; the solutions for which we

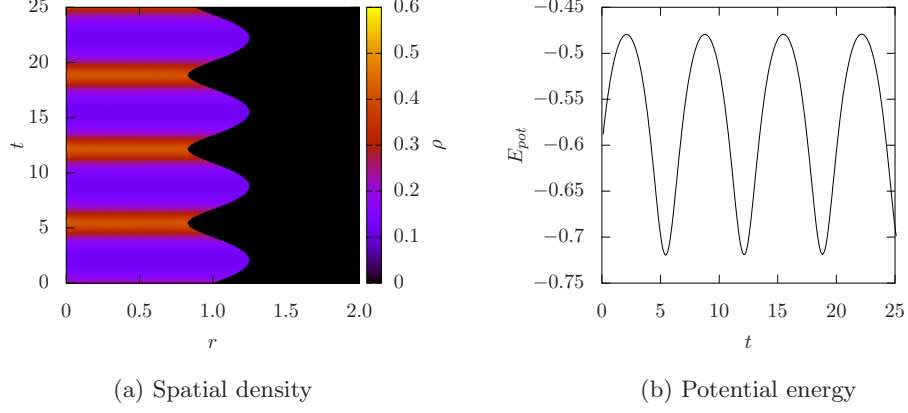


Figure 1: Time evolution of the Kurth solution with  $\epsilon = 0.2$ . The calculation used about  $36 \cdot 10^6$  particles.

want to conclude an oscillatory, time-periodic behavior from the numerical simulations are much smoother than the Kurth solutions.

Knowing that Kurth solutions are periodic in time, it is easy to determine their period from the previously shown results, but it is more involved to decide whether some periodic looking numerical result originates from a true periodicity of the underlying solution. To do so, we must in principle investigate the periodicity of the particle distribution function  $f$ , since the latter determines the dynamics and not some derived, macroscopic quantity like  $\rho$  or the kinetic or potential energy. To this end we use the fact that a continuous function  $\phi: \mathbb{R} \times \mathbb{R}^n \rightarrow \mathbb{R}$  is periodic in time with period  $T > 0$ , if it holds that

$$\|\phi(t, \cdot) - \phi(s, \cdot)\|_{L^1(\mathbb{R}^n)} = 0, \quad s = t + kT, \quad k \in \mathbb{Z}, \quad t \in \mathbb{R}.$$

We approximate the above norm by its discrete  $L^{1,h}$ -version, based on

$\epsilon$	0.1	0.2	0.3	0.4	0.5
$\lambda_e$	6.38	6.68	7.24	8.16	9.67
$\lambda_n$	6.39	6.70	7.24	8.16	9.66

Table 1: Exact  $\lambda_e$  and numerical  $\lambda_n$  periods of the Kurth solutions. The calculation used about  $33 \cdot 10^6 - 36 \cdot 10^6$  particles.

the particle discretisation used in our PIC code, and since we only have



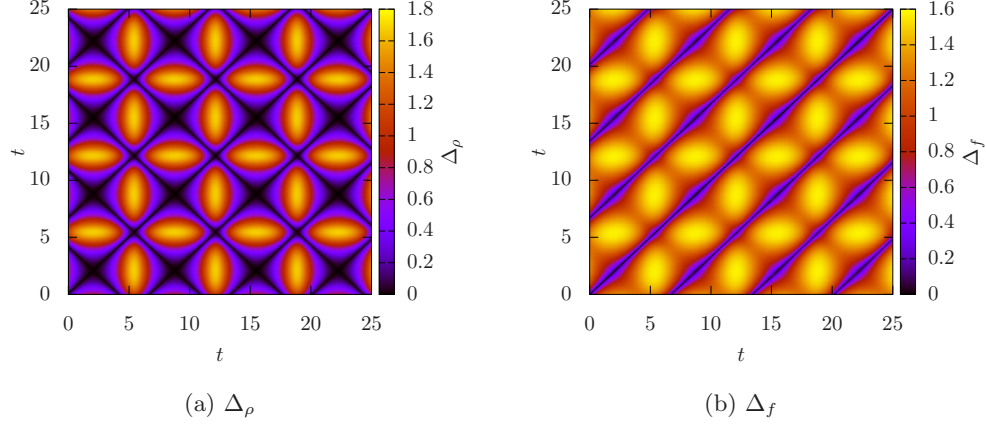


Figure 2:  $\Delta_\rho$  and  $\Delta_f$  for to the Kurth solution with  $\epsilon = 0.2$ . The calculation used about  $36 \cdot 10^6$  particles.

information on our approximation at a discrete set of times  $\mathcal{T} := \{t_j\}$ , we investigate the function

$$\Delta_f: \mathcal{T}^2 \rightarrow \mathbb{R}, \quad (t_i, t_j) \mapsto \|f(t_i, \cdot) - f(t_j, \cdot)\|_{L^{1,h}(\mathbb{R}^6)};$$

the function  $\Delta_\rho$  is defined in terms of  $\rho$  in the analogous way. The results are shown in Figures 2 (a) and (b). We see that there is a time  $T$  such that when  $t_i - t_j = kT$  for some integer  $k$  then both  $\Delta_f(t_i, t_j)$  and  $\Delta_\rho(t_i, t_j)$  become (almost) zero which indicates periodicity with period  $T$ . Notice that  $\Delta_\rho(t_i, t_j)$  also becomes (almost) zero when  $t_i + t_j = kT + s$  for some fixed  $s$ . This is due to the fact that  $\rho(T_0 + t) = \rho(T_0 - t)$  where  $T_0$  is one of the times when the state has maximal (or minimal) extension and  $t$  is arbitrary, cf. Figure 1 (a).

We now discuss the results obtained by perturbing the steady states mentioned above. The first thing one may ask is whether a Kurth-type perturbation applied to a different steady state again leads to a periodic solution. To begin with, we consider the polytropic shell with  $k = 1.0$ ,  $l = 0.5$ ,  $L_0 = 1.0$ , and  $y(0) = 1.0$ . Figure 3 shows the solutions triggered by Kurth-type perturbations with  $\epsilon = 0.05$  and  $\epsilon = 0.2$ , which appear to be (very close to) periodic. It is natural to ask, whether perturbations of different types launch solutions with a quasi-periodic behavior as well. It turns out that this is the case for most combinations of the perturbations and steady states mentioned above. Figure 4 shows a dynamically accessible perturbation of

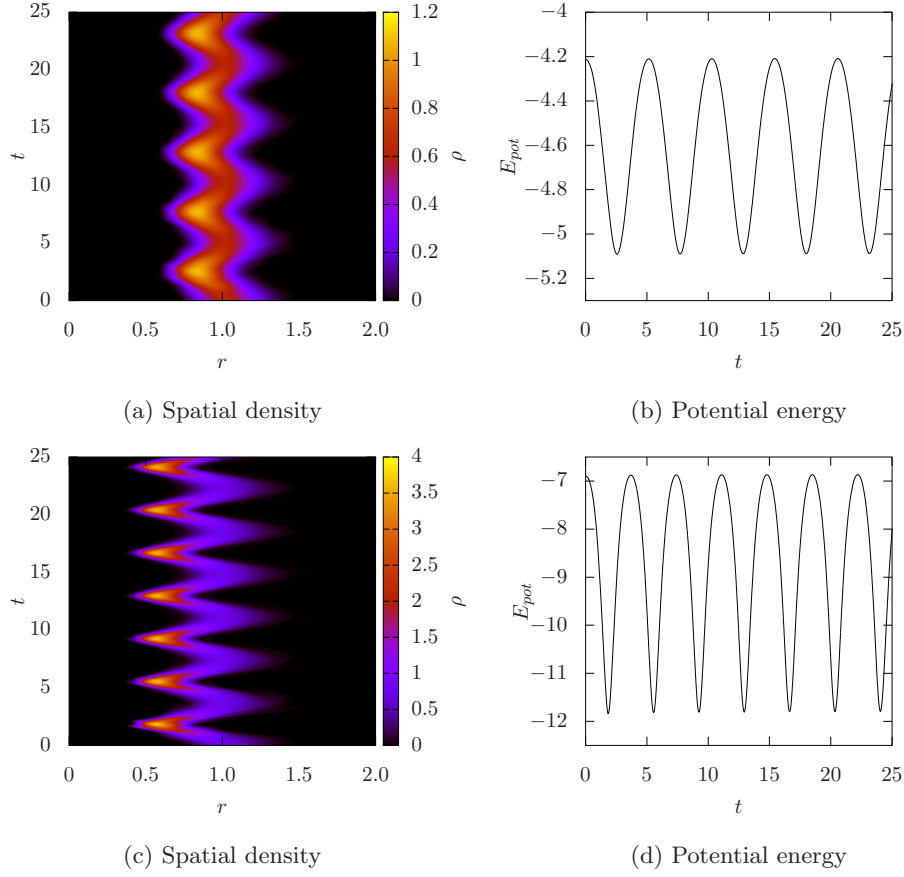


Figure 3: Shell for  $k = 1.0$ ,  $l = 0.5$  and  $L_0 = 1.0$  after a Kurth-type perturbation with  $\epsilon = 0.05$  (upper) and  $\epsilon = 0.2$  (lower) respectively.

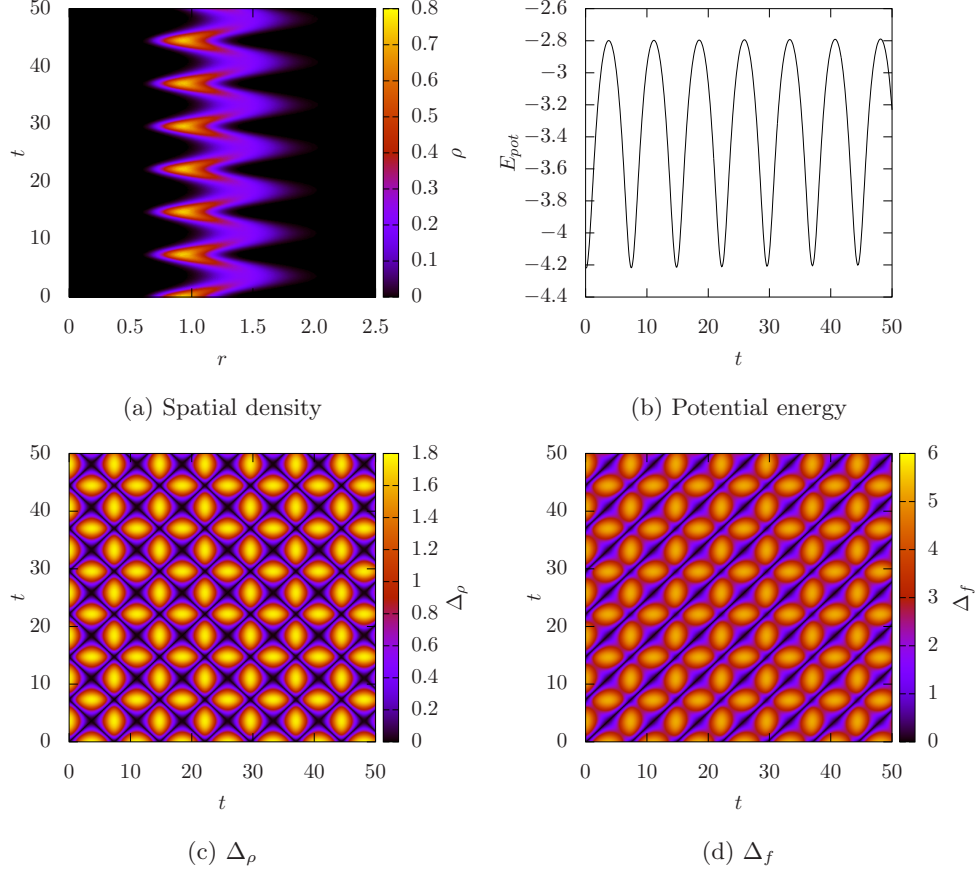


Figure 4: Shell solution with a dynamically accessible perturbation.

a shell solution, computed on a somewhat longer time interval. The figure also contains the potential energy and the functions  $\Delta_\rho$  and  $\Delta_f$  related to the solution.

It is worth mentioning that for a given steady state all the perturbations we applied to it led to oscillations of the same type. In particular, if the intensity of the perturbation, i.e., the amplitude of the oscillation, is reduced, then the period converges to a value which depends only on the specific steady state and not on the type of the perturbation. We were not able to find a clear numerical indication of different modes of the oscillations, but in Section 5 we report some observations which may be interpreted as superpositions of two different modes, cf. Figures 7 and 8. Figure 5 shows

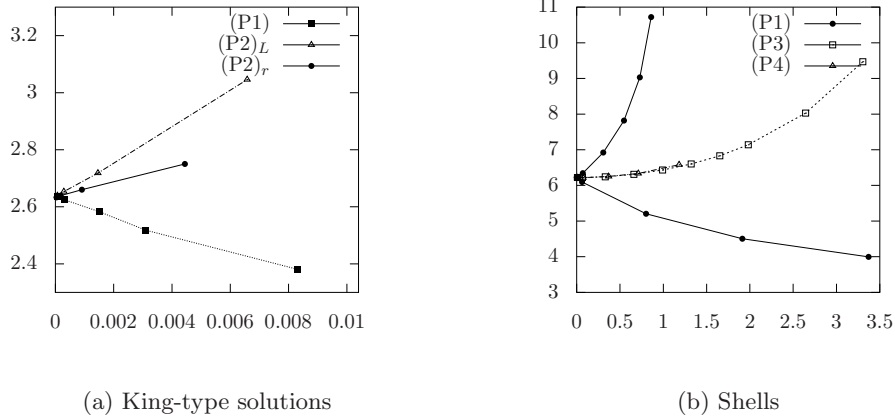


Figure 5: Relation of period and amplitude for different kinds of perturbations.

our results for one specific King and one specific shell solution.

## 4 The Eddington-Ritter relation

The light variations of the Cepheid variables can be explained by modelling them as time periodic pulsations of solutions to the Euler-Poisson system—for a review of the corresponding history we refer to [20]. Linearizing the Euler-Poisson system about a polytropic steady state Eddington [3] derived the following relation between the central density  $\rho(0)$  of the steady state and the period  $T$  of an oscillatory solution of the linearized system, triggered by a small perturbation of the steady state:  $\rho(0)^{1/2}T = \text{const}$ , where the constant depends on the parameters of the polytropic equation of state. Since such a relation was earlier suggested by Ritter, we refer to it as the *Eddington-Ritter relation*.

Isotropic steady states of the Vlasov-Poisson system are in one-to-one correspondence with those of the Euler-Poisson system with a suitable equation of state. For an isotropic state of the form (2.7) with  $l = 0$  the relation  $\rho(0) = c_k y(0)^{k+3/2}$  holds; we recall that a fixed ansatz function—in the present case fixed values for  $k$  and  $l$ —gives rise to a one-parameter family of steady states parameterized by  $y(0) = E_0 - U(0)$ . It is tempting to fix some  $k$  in (2.7) and determine numerically the quantity  $y(0)^{k/2+3/4}T$  for different choices of  $y(0)$ ;  $T$  is the period of the oscillation. In Table 2 and Table 3 this

$y(0)$	$T$	$c = y(0)^{3/4}T$
0.6	1.943	1.32451
0.8	1.569	1.32758
1.0	1.332	1.33214
1.2	1.167	1.33800
1.4	1.044	1.34364
1.6	0.947	1.34794

Table 2: Eddington-Ritter relation for  $k = 0$  and  $l = 0$

is done for  $k = 0$  and  $k = 1$  respectively. It should be noted that for  $k = 0$  the ratio of the maximal and minimal value for  $T$  equals  $T_{\max}/T_{\min} = 2.051$  while the ratio of the corresponding “constants” is  $c_{\max}/c_{\min} = 1.0177$ ; for  $k = 1$  we find  $T_{\max}/T_{\min} = 3.400$  and  $c_{\max}/c_{\min} = 1.003$ . Analogous result were found for different values of  $k$ . Hence one may indeed claim that an Eddington-Ritter relation does hold for the oscillations of galaxies. We should emphasize at this point that the periods in the tables above are obtained from simulations of oscillating solutions to the fully non-linear Vlasov-Poisson system which are triggered by small perturbations of the given steady state. For non-isotropic steady states of the Vlasov-Poisson

$y(0)$	$T$	$c = y(0)^{1/2+3/4}T$
0.6	5.233	2.76311
0.8	3.650	2.76157
1.0	2.761	2.76111
1.2	2.200	2.76312
1.4	1.815	2.76399
1.6	1.539	2.76922

Table 3: Eddington-Ritter relation for  $k = 1$  and  $l = 0$

system, for example states of the form (2.7) with  $l \neq 0$ , there do not exist corresponding steady states of the Euler-Poisson system. It is therefore an interesting question whether an Eddington-Ritter-type relation still holds for non-isotropic states, say, for states of the form (2.7) with  $l \neq 0$ . It is a-priori not obvious what the corresponding relation might be. In [7] the authors aim for a mathematical analysis of the oscillatory solutions to the Vlasov-Poisson system, and in the course of this investigation the relation

$$y(0)^{\frac{k+2l+3/2}{2l+2}}T = \text{const} \quad (4.1)$$

was formally derived, where the right hand side depends on  $k$  and  $l$ . We first observe that this relation reduces to the one which we checked numerically for the isotropic case  $l = 0$ . The results of a corresponding numerical check for the non-isotropic case  $k = 0$ ,  $l = 2$  are given in Table 4. In this case

$y(0)$	$T$	$c = y(0)^{\frac{4+3/2}{4+2}} T$
0.6	6.650	4.16352
0.8	5.113	4.16677
1.0	4.167	4.16731
1.2	3.529	4.17115
1.4	3.066	4.17320
1.6	2.717	4.17972

Table 4: Eddington-Ritter relation for  $k = 0$  and  $l = 2$

$T_{\max}/T_{\min} = 2.448$  while  $c_{\max}/c_{\min} = 1.0039$ .

In all the above numerical runs the system was evolved up to time 50 in  $3 \cdot 10^5$  time steps, using between  $19 \cdot 10^6$  and  $37 \cdot 10^6$  particles and dynamically accessible perturbations. The period was then determined from the fluctuations in the kinetic energy.

It seems fair to say that we have numerically verified (and in part analytically derived) an extension of the Eddington-Ritter relation to steady states of the Vlasov-Poisson system of polytropic form (2.7), including the non-isotropic case for which such a relation has no analogue in the fluid case.

## 5 Damping or no damping

In the above we have restricted ourselves to the gravitational case of the Vlasov-Poisson system. If the sign in the right hand side of the Poisson equation (1.2) is reversed, one obtains the plasma physics version of the system. In this case one can add a fixed, spatially homogeneous ion background, which then allows for spatially homogeneous and pointwise neutral steady states with vanishing electrostatic field. Based on an analysis by linearization L. LANDAU in 1946 predicted the phenomenon which was later termed “Landau damping”, whereby for small perturbations of these homogeneous equilibria the electrostatic field damps out to zero [11]. In the celebrated paper [16] the phenomenon of Landau damping was rigorously established on the non-linear level. In the gravitational case at hand the situation is more complicated, in particular, no spatially homogeneous steady states exist except for the vacuum state. Nevertheless, similar damping phenomena

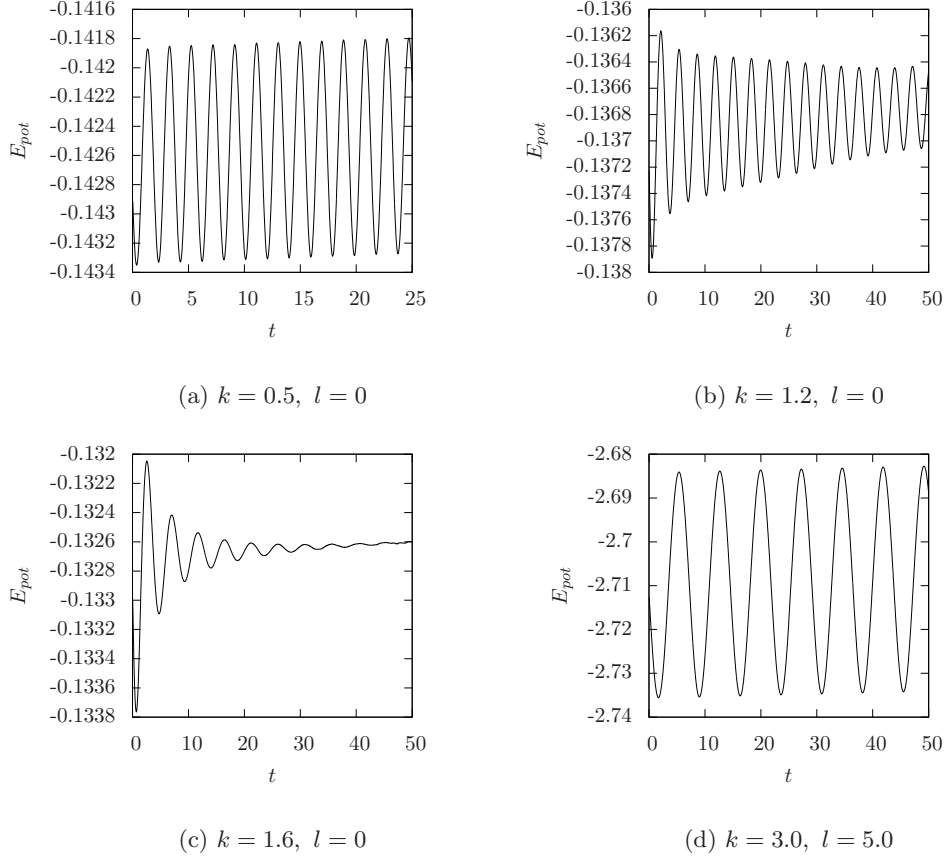


Figure 6: Damping phenomena.

are discussed in the astrophysics literature, cf. [2] and the references there or in [16]. The explicit solution family of KURTH, where exactly time periodic solutions are launched by small perturbations of a stationary one, shows that Landau damping need not always occur in the gravitational case.

Following [16], three ingredients seem important for Landau damping to happen: The perturbed steady state should be rather smooth, it should be spatially homogeneous or at least close to homogeneous on part of its support, and the perturbation should be sufficiently small.

In Figure 6 we plot the potential energy for a perturbation of a polytropic steady state for four different choices of  $k$  and  $l$ ; the perturbation is dynamically accessible, and about  $20 \cdot 10^6$  particles have been used. The

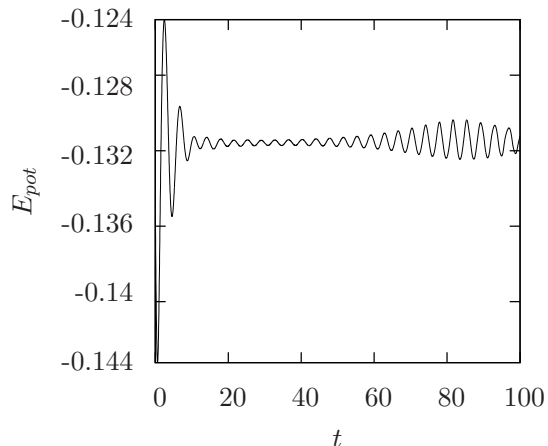


Figure 7:  $k = 1.6$ ,  $l = 0$  with a stronger perturbation.

first three plots show that with  $l = 0$  and increasing  $k$ , which corresponds to increasing smoothness of the steady state, the amplitude of the oscillation becomes more strongly damped. However, smoothness of the perturbed steady state alone is not sufficient for damping to take place. In Figure 6 (d) we perturb a polytropic state with  $k = 3$  and  $l = 5$ , which is smoother than the previous ones, but no damping is observed. A possible explanation is the fact that for  $l = 0$  the polytropic steady states have a strictly decreasing spatial density with  $\rho'(0) = 0$ , whereas  $l > 0$  leads to steady states with  $\rho(0) = 0$ , where  $\rho$  strictly increases up to some maximum and then strictly decreases. The latter behavior can be considered as more strongly inhomogeneous than the former. This also fits with the observation that no damping seems to occur for polytropic shells. It should be noted that in the examples above the perturbation is always rather small, as can be seen from the fact that initially the potential energy deviated only very little from its mean value.

In Figure 7 we again consider the fairly smooth isotropic polytrope  $k = 1.6$  and  $l = 0$ , but we consider a stronger perturbation. Had we stopped the computation at  $T = 20$ , this might have been tabbed as another example of a damped oscillation, but actually something quite different (and quite a bit more interesting) happens. A possible interpretation of this phenomenon



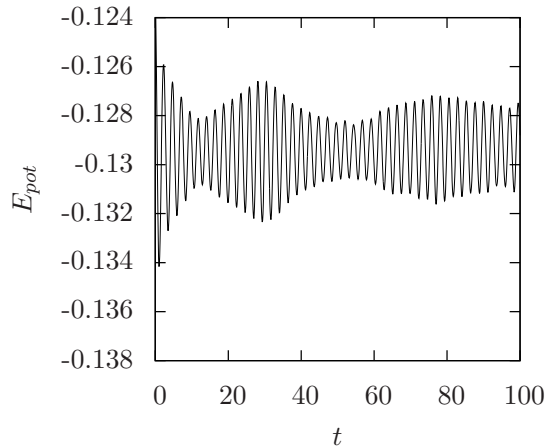


Figure 8: The King model with a stronger perturbation.

is that we here observe a superposition of two different oscillatory modes. In Figure 8 we see a similar effect as in Figure 7 for a perturbation of the King model, but we have so far not obtained a clear picture of the latter phenomenon, nor indeed of when oscillations are damped and when they are not.

## 6 Final comments

One should ask whether our numerical observations exhibit a genuine feature of the dynamics of the Vlasov-Poisson system or whether they are a numerical artefact. Firstly, it is easy to imagine that numerical effects destroy features like periodic orbits, but it seems hard to imagine that they generate these features. More importantly, for the Euler-Poisson system it is known by rigorous analysis that such time periodic oscillations exist on the linearized level and that in a well-defined sense they approximately survive for the non-linear system, cf. [3, 8, 15, 20]. The fact that we recover the Eddington-Ritter relation, which is known in the Euler-Poisson context, also in the Vlasov-Poisson context and that in [7] a formal derivation of this relation from a suitable linearized system is obtained is a strong indication that the observed oscillations are a genuine feature of the Vlasov-Poisson

dynamics.

Finally, one should ask whether our numerical observations are relevant for astrophysics. In this context it seems of interest to express the observed periods in suitable units. By matching the numerically obtained values for the radius and mass of a given steady state with observed data for a real galaxy we fix the units of length and mass. Moreover, the Vlasov-Poisson system contains only one physical constant, namely the gravitational constant, which we have set to unity. This in turn fixes the unit of time and allows us to turn the numerical values for the period of the oscillations into values with proper units. The diameter of elliptical galaxies, which can be close to spherically symmetric and are thus of interest here, ranges between 0.1 kpc and 100 kpc and their mass between  $10^7$  and  $10^{13}$  solar masses. The oscillation period predicted from a polytropic model with  $k = 1, l = 0$  and  $y(0) = 0.6$  ranges between  $1.7 \cdot 10^7$  years for “small” galaxies and  $5.4 \cdot 10^8$  years for “large” ones;  $k = 1, l = 0$  and  $y(0) = 1.6$  yields  $1.1 \cdot 10^7$  years for “small” and  $3.4 \cdot 10^8$  years for “large” galaxies. Of course these numbers change with the steady state model, but we found that the time scale of  $10^7 - 10^8$  years seems typical, and it seems to be of an astrophysically reasonable order of magnitude.

The analogous oscillations for the Euler-Poisson system were used to explain for example the Cepheid variables, cf. [3]. It should also be noted that many arguments in the astrophysical analysis of galaxies explicitly or implicitly rely on the assumption that they are in some equilibrium. It seems debatable how justified this assumption is. In any case, the question whether galaxies can oscillate has been asked in the astrophysics literature, cf. [14], and if one models galaxies by the Vlasov-Poisson system, then the answer to this question should be an emphatic “Yes”.

## References

- [1] ANDRÉASSON, H., REIN, G. A numerical investigation of the stability of steady states and critical phenomena for the spherically symmetric Einstein-Vlasov system, *Class. Quantum Grav.* **23**, 3659–3677 (2006).
- [2] BINNEY, J., TREMAINE, S., *Galactic Dynamics*, Princeton University Press, Princeton 1987.
- [3] EDDINGTON, A., On the pulsations of a gaseous star and the problem of the Cepheid variables, Part I, *Monthly Notices Royal Astr. Soc.* **79**, 2–22 (1918).

- [4] GUO, Y., Variational method in polytropic galaxies. *Arch. Rational Mech. Anal.* **150**, 209–224 (1999).
- [5] GUO, Y., REIN, G., Isotropic steady states in galactic dynamics. *Commun. Math. Phys.* **219**, 607–629 (2001).
- [6] GUO, Y., REIN, G., A non-variational approach to nonlinear stability in stellar dynamics applied to the King model. *Commun. Math. Phys.* **271**, 489–509 (2007).
- [7] HADŽIĆ, M., REIN, G., On the analysis of oscillating solutions of the Vlasov-Poisson system. *In preparation*.
- [8] JANG, J., Time periodic approximations of the Euler-Poisson system near Lane-Emden stars. *Preprint* (2015).
- [9] KORCH, M., RAMMING, T., REIN, G. Parallelization of particle-in-cell codes for nonlinear kinetic models from mathematical physics. *Proceedings of the 2013 International Conference on Parallel Processing (ICPP 2013)*, 523–529 (2013).
- [10] KURTH, R., A global particular solution to the initial-value problem of stellar dynamics. *Quart. Appl. Math.*, **36**, 325–329 (1978).
- [11] LANDAU, L., On the vibrations of the electronic plasma. *Akad. Nauk SSSR. Zhurnal Eksper. Teoret. Fiz.* **16**, 574–586 (Russian, 1946); English translation in *Acad. Sci. USSR. J. Phys.*, **10** (1946).
- [12] LEMOU, M., MÉHATS, F., RAPHAËL, P., Orbital stability of spherical galactic models. *Invent. math.* **187**, 145–194 (2012).
- [13] LIONS, P.-L., PERTHAME, B., Propagation of moments and regularity for the 3-dimensional Vlasov-Poisson system, *Invent. Math.* **105**, 415–430 (1991).
- [14] LOUIS, P., GERHARD, O., Can galaxies oscillate? A self-consistent model of a non-stationary stellar system. *Monthly Notices Royal Astr. Soc.* **233**, 337–365 (1988).
- [15] MAKINO, T., On spherically symmetric motions of a gaseous star governed by the Euler-Poisson system, *Osaka J. Math.* **52**, 545–580 (2015).
- [16] MOUHOT, C., VILLANI, C., On Landau damping, *Acta Math.* **207**, 29–201 (2011).

- [17] PFAFFELMOSER, K., Global classical solutions of the Vlasov-Poisson system in three dimensions for general initial data. *J. Differential Equations* **95**, 281–303 (1992).
- [18] RAMMING, T., REIN, G., Spherically symmetric equilibria for self-gravitating kinetic or fluid models in the non-relativistic and relativistic case—A simple proof for finite extension. *SIAM J. on Mathematical Analysis* **45**, 900–914 (2013).
- [19] REIN, G., Collisionless kinetic equations from astrophysics—The Vlasov-Poisson system. In *Handbook of Differential Equations, Evolutionary Equations, vol. 3*, ed. by C. M. Dafermos and E. Feireisl, Elsevier (2007).
- [20] ROSSELAND, S., George Darwin Lecture: The pulsation theory of Cepheid variables. *Monthly Notices Royal Astr. Soc.* **103**, 233–243 (1943).
- [21] SCHAEFFER, J., Global existence of smooth solutions to the Vlasov-Poisson system in three dimensions *Comm. Partial Differential Equations* **16**, 1313–1335 (1991).